JOURNAL OF SOLID STATE CHEMISTRY **44**, 291–297 (1982)

Kinetics and Mechanism of the Solid-State Reaction $Cu_2Mo_3O_{10} + \frac{1}{2} O_2 \rightarrow 2CuMoO_4 + MoO_3$

J. HABER AND K. JAMROŻ

Institute of Catalysis and Surface Chemistry, Polish Academy of Sciences, Kraków, Poland

Received June 23, 1981; in revised form April 26, 1982

Kinetics of the solid-state reaction $Cu_2Mo_3O_{10} + \frac{1}{2}O_2 \rightarrow 2CuMoO_4 + MoO_3$ were determined as a function of temperature and oxygen pressure. At oxygen pressures higher than 11 Torr nucleation of $CuMoO_4$ is the rate-determining step, the kinetic curves conforming to affine transformations. At lower oxygen pressures the reaction is reversible, probably limited to the surface layer only.

Reactions of oxidation and reduction of transition metal oxides and their oxysalts have in recent years been a subject of considerable interest because of their importance as models for studying the correlation between the kinetics and the mechanism of solid-state reactions on the one hand and because of their significance for understanding the catalytic activity of these oxides in selective oxidation on the other.

Reactions of the selective oxidation of organic molecules proceed with the redox mechanism, lattice oxygen ion from the catalyst being inserted into the organic molecule and the catalyst then being reoxidized by oxygen from the gas phase. In the steady-state conditions a certain degree of reduction of the catalyst is established, depending on the ratio of the rate of reduction of the solid to the rate of its reoxidation. Information on the kinetics and mechanism of the reduction and reoxidation of such systems is therefore of considerable interest.

Recently it was shown (*1–3*) that, in the case of such systems as copper molybdates, the transformations between Cu(I) and Cu(II) structures have a profound influence not only on the catalytic activity but also on the selectivity of the formation of products obtained as the result of the oxidation of hydrocarbons. It therefore seemed interesting to study the kinetics and mechanism of the reaction

$$\tfrac{1}{2}Cu^{I}_{2}Mo^{VI}_{3}O_{10} + O_2 \rightarrow Cu^{II}Mo^{VI}O_4 + Mo^{VI}O_3, \quad (1)$$

the three solid phases being known as components of the copper molybdate catalysts for selective oxidation.

Experimental

$Cu_2Mo_3O_{10}$ was prepared by solid-state reaction between Cu_2O and MoO_3:

$$Cu_2O + 3MoO_3 \rightarrow Cu_2Mo_3O_{10}. \quad (2)$$

The starting materials were commercial products of analytical grade. $Cu_2Mo_3O_{10}$ was obtained by heating the initial mixture of Cu_2O and MoO_3 in stoichiometric ratio in sealed evacuated quartz ampoules at 520°C

0022-4596/82/120291-07$02.00/0

for 20 hr. The details of the preparation and properties of $Cu_2Mo_3O_{10}$ have been described in (*4–6*). X-Ray analysis of the samples obtained indicates that the only product of the reaction is $Cu_2Mo_3O_{10}$. Its surface area, determined by standard BET gas adsorption technique with krypton as the adsorbate, was found to be 1.3 m^2/g.

Kinetics of the $Cu_2Mo_3O_{10}$ oxidation were studied by monitoring the changes of the weight of the sample using a Cahn Model RG electrobalance with 10^{-5} accuracy. The microbalance was connected to the conventional vacuum system, which enabled oxygen to be introduced on the sample at pressures between 1×10^{-5} and 760 Torr. The sample and reference weight were heated by two temperature-programmed furnaces. The temperature controller maintained the temperature constant to within ±1°C during the isothermal experiments. The temperature of the sample was continuously monitored by a Cr–NiCr thermocouple suspended near the sample inside the tube.

Adsorption of oxygen on $Cu_2Mo_3O_{10}$ samples was studied in a conventional volumetric system.

The preliminary oxidation experiments revealed that the rate of oxidation is independent of the sample mass for samples not exceeding 0.2 g. Thus samples of about 0.1 g were used in all the thermogravimetric experiments. In order to increase the sensitivity in the adsorption measurements samples of about 2 g of $Cu_2Mo_3O_{10}$ were used in the volumetric experiments.

Oxidation was carried out in pure oxygen obtained by fractional distillation of liquid air. The conditions of standardization were as follows: all samples were outgassed until a pressure of 5×10^{-5} Torr was obtained, then heated to 425°C, outgassed during 0.5 hr, and cooled to the temperature of the experiment. Experiments were carried out within the temperature range 250–390°C. Products formed as the result of the oxidation of $Cu_2Mo_3O_{10}$ were identified by X-ray powder diffraction method.

Results and Discussion

Prior to the studies of the oxidation kinetics a series of adsorption experiments at low oxygen pressure were carried out in order to find out whether oxidation is preceded by adsorption of oxygen at the surface of the $Cu_2Mo_3O_{10}$ crystallites. No adsorption was observed at temperatures below 200°C. Above this temperature a continuous uptake of oxygen took place, with the amount of oxygen consumed increasing linearly with time as illustrated in Fig. 1. The amount which would correspond to a close-packed monolayer coverage of the surface by oxygen is shown by the dotted line. It may be concluded that the oxygen uptake observed in these experiments is due to the oxidation of the solid substrate, which is not preceded by any rapid adsorption.

Figure 2 shows the degree of conversion α calculated according to Eq. (1) as a function of time for the reaction carried out at 350°C at different oxygen pressures between 11 and 150 Torr, and Fig. 3 shows the degree of conversion α as a function of time for the reaction carried out at 40 Torr of oxygen and different temperatures between 273 and 390°C. All $\alpha_T(p,t)$ curves as well as $\alpha_p(T,t)$ curves conform to the affine transformations, i.e.,

$$\alpha_T(p_i,t) \rightarrow \alpha_T(p_j,b_i^j t),$$
$$\alpha_p(T_m,t) \rightarrow \alpha_p(T_n,b_m^n t),$$

where b_i^j and b_m^n are constants. When this is the case, the variables in the rate equation

$$\frac{d\alpha}{dt} = r(T,p,x_i,\alpha) \qquad (3)$$

can be separated into two functions:

$$\frac{d\alpha}{dt} = k(T,p,x_i) \cdot f(\alpha) \qquad (4)$$

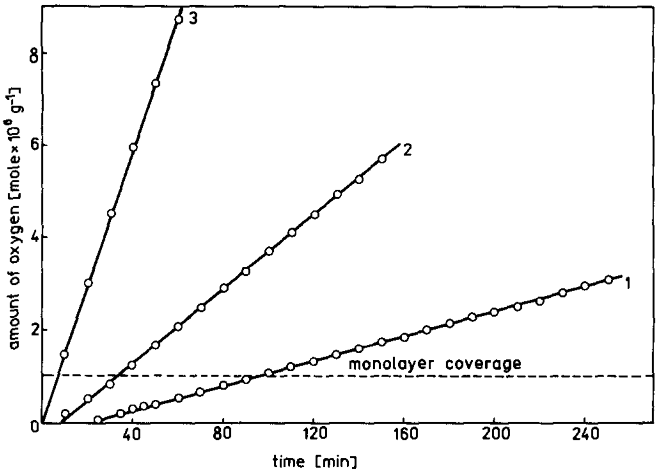

FIG. 1. The amount of oxygen consumed as a function of time at p_{O_2} = 3.5 Torr. 1, 200°C; 2, 250°C; 3, 315°C.

This indicates that the series of states traversed by the system is invariant with respect to intensive variables such as temperature or pressure. These states are attained at times that are all multiplied by *b*. Thus the texture and structure of the reaction products are independent of the temperature and oxygen pressure above 11 Torr.

The conformity of the kinetic curves to affine transformations is an obligatory but not sufficient condition for a single step to be determining the rate of the reaction. In such a case the kinetic curve can be described by a single equation, valid for all degrees of conversion, with the rate constant depending only on intensive parameters. The form of this equation can supply information concerning which of the steps is controlling the overall rate of the reaction. Many solid-state reactions can be described by equations of the type $F(\alpha) = kt$, where the function $F(\alpha)$ depends on the

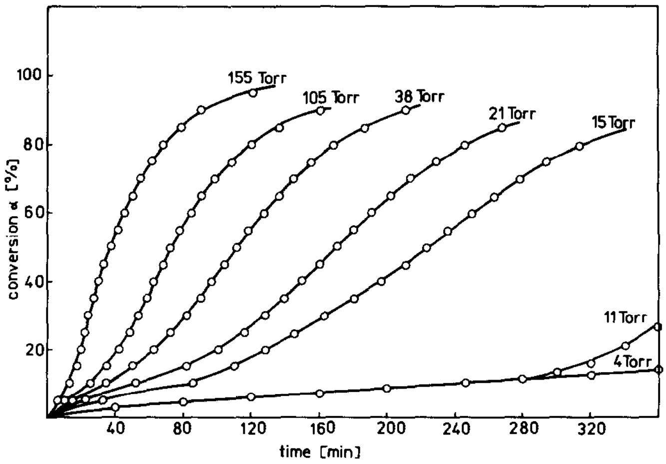

FIG. 2. Degree of oxidation of $Cu_2Mo_3O_{10}$ in oxygen at 350°C as a function of time at different pressures.

mechanism controlling the reaction, as well as the size and shape of the reacting particles. These equations may be divided into four groups:

1. Diffusion-controlled,
2. Equations based on the concept of the order of reaction,
3. Phase-boundary controlled,
4. Nucleation and nuclei growth.

Table I presents the equations considered (*7–10*). The functions $D_1(\alpha)$ through $D_4(\alpha)$ represent some of the most important diffusion equations. $F_0(\alpha)$ and $F_1(\alpha)$ are the functions for zero and first-order reactions.

If a reaction is controlled by movement of an interface, it can be described using $R_2(\alpha)$ and $R_3(\alpha)$ equations.

When nucleation and nuclei growth processes are rate-determining, Eqs. $A_2(\alpha)$ and $A_3(\alpha)$ are usually used. In comparing experimental data it is usually convenient to use a reduced time scale, such as $t/t_{0.5}$, where $t_{0.5}$ corresponds to $\alpha = 0.5$.

Comparison of experimental kinetic data for the $Cu_2Mo_3O_{10}$ oxidation with those calculated theoretically shows that agreement is obtained only with equations based on nucleation and nuclei growth.

The phenomenological theory of nucleation and growth takes into account two different parallel processes taking place in a reacting system: the growth of nuclei already formed and the appearance of new ones. At a certain value of α, the crystal nuclei of product get into contact with each other. From this moment the overlapping of the product nuclei takes place and a decrease of the reaction rate $d\alpha/dt$ is observed.

Rate equations of the form $F(\alpha) = kt$ are derived through integrations of specific forms of the generalized expression representing the summation of the growth of all nuclei, so that the volume of product at time t, $V(t)$, is given by

$$V(t) = \int_0^t V(t,t_j)\left(\frac{dN}{dt}\right)_{t_j} dt_j. \tag{5}$$

This may be integrated for any combination of the law of nucleation (the dN/dt term) and the law of growth (the $V(t,t_j)$ term).

Avrami (*11*), Erofeev (*12*), Mampel (*13*), and recently Delmon (*14*) derived in different ways the equation

$$[-\ln(1-\alpha)]^{1/n} = k(t - t_0), \tag{6}$$

often referred to as the Avrami–Erofeev equation.

Plots of $\ln[-\ln(1-\alpha)]$ vs $\ln t$ are shown in Fig. 4. A linear dependence with slopes equal to 2 is obtained, indicating that the reaction proceeds through the flat nuclei.

Figure 5 shows the dependence of the rate of reaction on the pressure. Two pressure ranges can be distinguished: pressures above 11 Torr, in which the reaction is of first order with respect to oxygen, and the range below this pressure, in which the reaction is of zero order. The former is the range of validity of Eq. (6).

An Arrhenius plot of the reaction rates is shown in Fig. 6. The activation energy for

TABLE I

RATE EQUATIONS CHECKED FOR OXIDATION OF $Cu_2Mo_3O_{10}$

Function	Equation	Function	Equation
$D_1(\alpha)$	$\alpha^2 = kt$	$F_1(\alpha)$	$-\ln(1-\alpha) = kt$
$D_2(\alpha)$	$(1-\alpha)\ln(1-\alpha) + \alpha = kt$	$R_2(\alpha)$	$1-(1-\alpha)^{1/2} = kt$
$D_3(\alpha)$	$[1-(1-\alpha)^{1/3}]^2 = kt$	$R_3(\alpha)$	$1-(1-\alpha)^{1/3} = kt$
$D_4(\alpha)$	$1 - 2\alpha/3 - (1-\alpha)^{2/3} = kt$	$A_2(\alpha)$	$[-\ln(1-\alpha)]^{1/2} = kt$
$F_0(\alpha)$	$\alpha = kt$	$A_3(\alpha)$	$[-\ln(1-\alpha)]^{1/3} = kt$

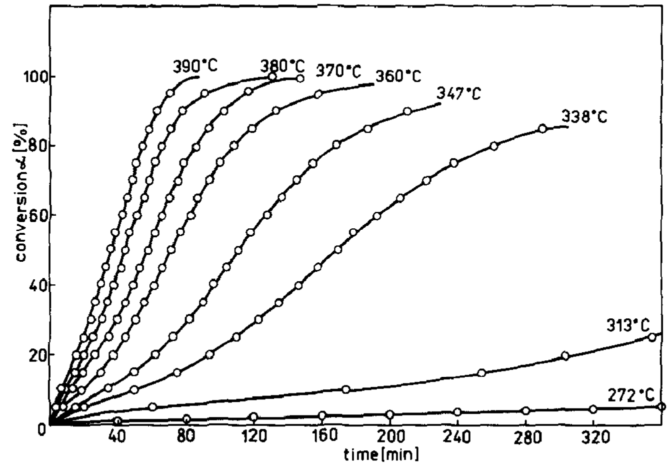

FIG. 3. Degree of oxidation of $Cu_2Mo_3O_{10}$ in 40 Torr of oxygen as a function of time at different temperatures.

the reaction is 18.3 ± 0.5 kcal · $mole^{-1}$. Figure 7 shows no change in the activation energy with degree of conversion.

Thus, at oxygen pressures higher than 11 Torr, kinetics of the reaction may be described by the rate equation

$$-\ln (1 - \alpha) = k(t - t_0)^2, \qquad (7)$$

in which

$$k = k_0 \cdot p_{O_2} \cdot \exp(-\Delta E/RT), \qquad (8)$$

indicating that nuclei growth is the rate-determining step. The first-order dependence

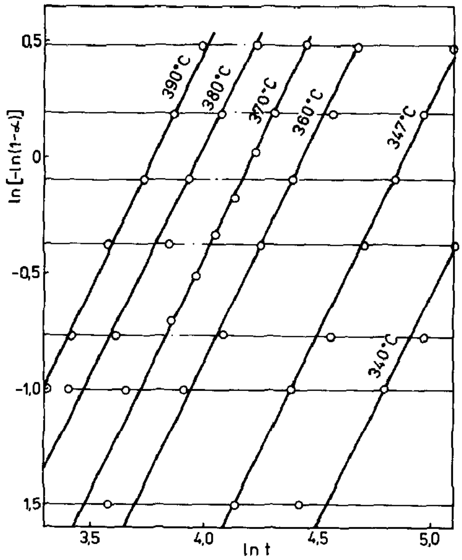

FIG. 4. ln [−ln (1 − α)] as a function of ln time for oxidation of $Cu_2Mo_3O_{10}$ in 40 Torr of oxygen.

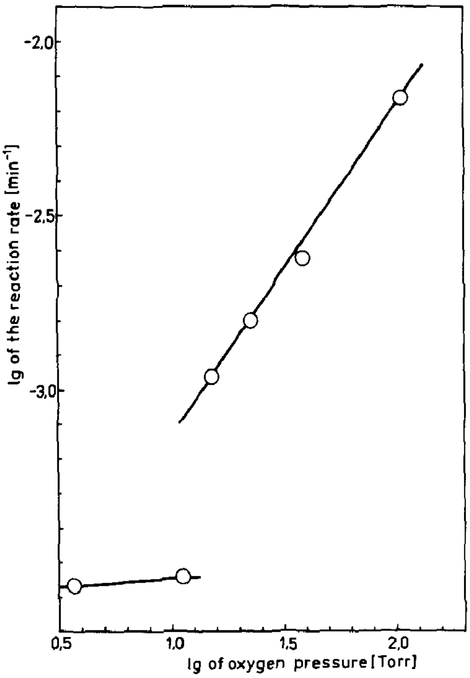

FIG. 5. Dependence of the rate of reaction on the oxygen pressure at 350°C.

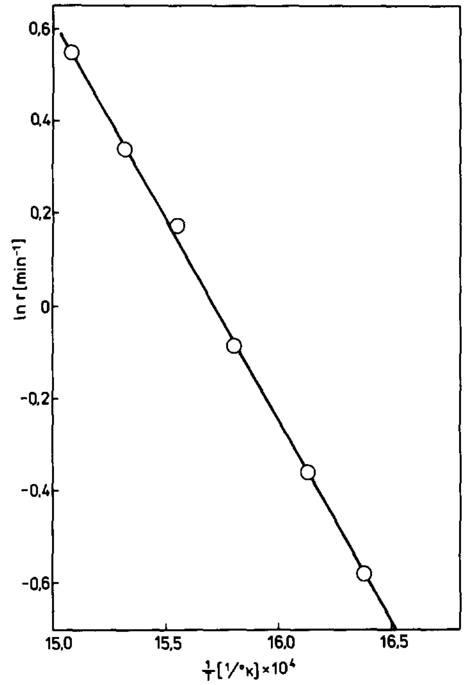

FIG. 6. Arrhenius plot of the reaction carried out at 40 Torr of oxygen.

on oxygen pressure reflects the chemical process involved in the growth of product nuclei as described by Eq. (2).

In order to confirm this conclusion and to establish which product is most difficult to form, experiments were carried out in which the rates of the oxidation of $Cu_2Mo_3O_{10}$ with small additions of $CuMoO_4$, MoO_3, or both $CuMoO_4$ and MoO_3 were measured.

Figure 8 indicates that the oxidation process is accelerated by the addition of 1 wt% of $CuMoO_4$, whereas its rate is practically independent of the addition of MoO_3.

Thus it may be concluded that the formation and growth of $CuMoO_4$ nuclei is the rate-controlling step.

Below the pressure of 11 Torr of oxygen a linear dependence of the conversion on time was observed:

$$\alpha = k't. \tag{9}$$

This rate law was obeyed during all investigated times of the reaction, which in one experiment amounted to as long as 1180 min, and the rate was independent of oxygen pressure (cf. Fig. 5). This implies that in the oxygen pressure range below 11 Torr the rate-determining step of the reaction is nucleation which may be described by the linear rate equation.

In order to obtain more information about the mechanism of the oxidation at low oxygen pressures a series of oxidation–reduction measurements were carried out. A sample of $Cu_2Mo_3O_{10}$ was oxidized at the temperature of 350°C and under oxygen pressure equal to 9.6 Torr. When the conversion α reached 0.092 oxidation was stopped and the sample was reduced in 15 Torr of hydrogen at T = 380°C until the mass of the sample decreased to the initial value. The oxidation–reduction cycle was repeated, the kinetics of the oxidation and reduction were measured gravimetrically, and X-ray analysis of the oxidized and reduced samples was carried out. It was found that the structure of the sample after

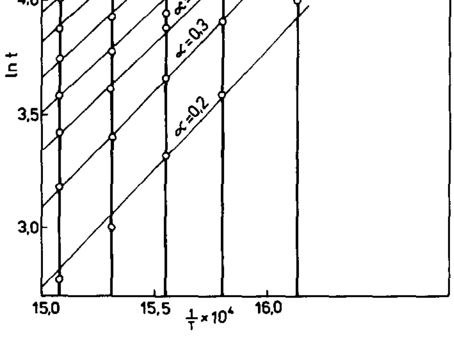

FIG. 7. Logarithm of time of the given conversion as a function of reciprocal temperature for different conversions at 40 Torr of oxygen.

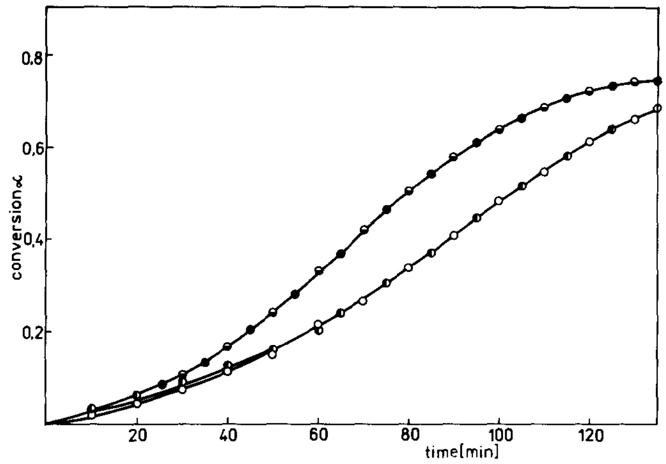

FIG. 8. Degree of oxidation in 40 Torr of oxygen at 350°C:
—pure $Cu_2Mo_3O_{10}$,
—$Cu_2Mo_3O_{10}$ with 1 wt% of $CuMoO_4$,
—$Cu_2Mo_3O_{10}$ with 1 wt% of MoO_3,
—$Cu_2Mo_3O_{10}$ with 1 wt% of $CuMoO_4$ and MoO_3 (1 : 1).

the oxidation–reduction cycle is identical to the structure of the initial $Cu_2Mo_3O_{10}$, and the kinetics of the oxidation of the former do not differ from those of the fresh $Cu_2Mo_3O_{10}$. Thus the oxidation–reduction–reoxidation cycles of $Cu_2Mo_3O_{10}$ under these conditions are reversible and the crystal structure of the bulk of the sample does not change.

It should, however, be emphasized that reaction (1) is irreversible, because reduction of $CuMoO_4$ gives a mixture of $Cu_2Mo_3O_{10}$ and $Cu_6Mo_4O_{15}$. Thus it must be assumed that the observed reversibility of the oxidation of $Cu_2Mo_3O_{10}$ at low oxygen pressures is due to the fact that in the first stage of the reaction bidimensional oxidized surface phases are formed, the growth of nuclei of the $CuMoO_4$ phase taking place only in the more advanced stage of the reaction, e.g., at higher oxygen pressures. This conclusion is consistent with the results of photoelectron spectroscopic studies of the changes of surface structure of $Cu_2Mo_3O_{10}$ in the course of the catalytic oxidation of hydrocarbons [2].

References

1. J. HABER AND T. WILTOWSKI, *Bull. Acad. Pol. Sci. Ser. Sci. Chim.* **27**, 785 (1979).
2. J. HABER, J. STOCH, AND T. WILTOWSKI, *React. Kinet. Catal. Lett.* **13**, 161 (1980).
3. J. HABER, J. STOCH, AND T. WILTOWSKI, "Proceedings, 7th International Congress on Catalysis, Tokyo, 1980," in press.
4. T. MACHEJ AND J. ZIÓŁKOWSKI, *Bull. Acad. Pol. Sci. Ser. Sci. Chim.* **24**, 577 (1976).
5. T. MACHEJ AND J. ZIÓŁKOWSKI, *J. Solid State Chem.* **37**, 135 (1980).
6. J. HABER, T. MACHEJ, L. UNGIER, AND J. ZIÓŁKOWSKI, *J. Solid State Chem.* **25**, 207 (1978).
7. J. H. SHARP AND G. W. BRINDLEY, *J. Amer. Ceram. Soc.* **49**, 379 (1966).
8. J. D. HANNOCK AND J. H. SHARP, *J. Amer. Ceram. Soc.* **55**, 74 (1972).
9. R. A. GARDNER, *J. Solid State Chem.* **9**, 336 (1974).
10. M. SETVERATNARU AND P. D. GARU, *J. Amer. Ceram. Soc.* **59**, 376 (1976).
11. M. AVRAMI, *J. Chem. Phys.* **7**, 1103 (1939); **8**, 212 (1940); **9**, 177 (1941).
12. B. V. EROFEEV, *Dokl. Acad. Sci. USSR* **52**, 511 (1946).
13. K. L. MAMPEL, *Z. Phys. Chem. Abt. A* **187**, 43, 235 (1940).
14. B. DELMON, "Introduction a la Cinetique Heterogene," Technip, Paris (1969).